文章编号:1001 - 9014(2011)06 - 0481 - 05

High indium content InGaAs photodetector: with InGaAs or InAlAs graded buffer layers

GU Yi[1,3], WANG Kai[1,2], LI Cheng[1,2], FANG Xiang[1,2],
CAO Yuan-Ying[1,2], ZHANG Yong-Gang[1,3*]

(1. State Key Laboratory of Functional Materials for Informatics, Shanghai Institute of Microsystem and Information Technology, Chinese Academy of Sciences, Shanghai 200050, China;
2. Graduate School of Chinese Academy of Sciences, Beijing 100039, China;
3. Key Laboratory of Infrared Imaging Materials and Detectors, Chinese Academy of Sciences, Shanghai 200083, China)

Abstract: High indium content $In_{0.78}Ga_{0.22}As$ photodetector structures have been grown on InP substrates with $In_xGa_{1-x}As$ or $In_xAl_{1-x}As$ graded buffer layers wherein x changed continuously by gas source molecular beam epitaxy. Their characteristics were investigated by atomic force microscope, x-ray diffraction, transmission electron microscopy and photoluminescence. The differences between samples with the two kinds of buffer layers were studied. Results show that moderate surface morphology can be obtained with either $In_xGa_{1-x}As$ or $In_xAl_{1-x}As$ buffer layers. Larger residual strain is present in the photodetector structure with $In_xGa_{1-x}As$ buffer layer. On the other hand, superior optical characteristics have been observed for the photodetector structure with $In_xAl_{1-x}As$ buffer layer.

Key words: photodetector; high indium content; buffer; InGaAs; InAlAs
PACS: 81.05.Ea, 81.15.Hi, 78.55.Cr, 61.05.cp

采用 InGaAs 或 InAlAs 缓冲层的高 In 组分 InGaAs 探测器结构材料特性

顾 溢[1,3], 王 凯[1,2], 李 成[1,2], 方 祥[1,2], 曹远迎[1,2], 张永刚[1,3,*]

(1. 中国科学院上海微系统与信息技术研究所 信息功能材料国家重点实验室, 上海 200050;
2. 中国科学院研究生院, 北京 100039; 3. 中国科学院红外成像材料与器件重点实验室, 上海 200083)

摘要: 利用气态源分子束外延在 InP 衬底上生长了具有 $In_xGa_{1-x}As$ 或 $In_xAl_{1-x}As$ 连续递变缓冲层的高 In 组分 $In_{0.78}Ga_{0.22}As$探测器结构. 通过原子力显微镜、X 射线衍射、透射电子显微镜和光致发光对它们的特性进行了表征和比较. 结果表明, 具有 $In_xGa_{1-x}As$ 或 $In_xAl_{1-x}As$ 缓冲层的结构都能获得较平整的表面; 具有 $In_xGa_{1-x}As$ 缓冲层的探测器结构表现出更大的剩余应力; 具有 $In_xAl_{1-x}As$ 缓冲层的探测器结构所观察到的光学特性更优.

关 键 词: 光电探测器; 高 In 组分; 缓冲层; InGaAs; InAlAs
中图分类号: TN2 **文献标识码**: A

Introduction

There are many important applications for the photodetectors (PDs) with response wavelength between 1 to 3 μm. Ternary InGaAs absorption layer is an alternative in this band to HgCdTe or antimonide. $In_{0.53}Ga_{0.47}As$ PDs lattice-matched to the InP substrate with bandgap wavelength of about 1.7 μm have been well

Received date: 2011 - 02 - 17, **revised date**: 2011 - 06 - 14 **收稿日期**: 2011 - 02 - 17, **修回日期**: 2011 - 06 - 14
Foundation items: Natural Science Foundation of Shanghai (10ZR1436300); Innovative Foundation of Shanghai Institute of Microsystem and Information Technology; Foundation of Key Laboratory of Infrared Imaging Materials and Detectors CAS.
Biography: GU Yi, (1982-), male, Jiangsu, assistant researcher, research area is semiconductor optoelectronic materials and devices. E-mail: ygu@mail.sim.ac.cn.
* **Corresponding author**: E-mail: ygzhang@mail.sim.ac.cn.

developed mainly for the fiber communication applications. By increasing the indium (In) content of the InGaAs alloy, while the bandgap wavelength is red shifted, a quite large lattice mismatch between InGaAs layer and InP substrate is introduced unavoidably. In the high In content PD structures, a suitable buffer layer between InP substrate and InGaAs layer should be inserted to prevent the propagation of threading dislocations and degradation of the material quality. Many efforts have been made on the schemes of the buffer layers, such as linear graded buffer [1-2], step graded buffer [3] and superlattice buffer [4]. By molecular beam epitaxy (MBE) technology, the $In_xGa_{1-x}As$ or $In_xAl_{1-x}As$ continuously graded buffer layers are feasible schemes because of the convenient composition control of group III sources [5]. Comparing $In_xGa_{1-x}As$ with $In_xAl_{1-x}As$ graded buffer layers, InAlAs heterojunction buffer with wider bandgap should be more appropriate for the device performances and the applications of focal plane array, whereas InGaAs homojunction buffer is generally considered with better material quality if only from the material point of view. In this work, our interests focus on the comparison of material quality for InP-based high In content InGaAs PD structures on $In_xGa_{1-x}As$ or $In_xAl_{1-x}As$ graded buffer layers by the investigation of their surface morphology, structural and optical qualities.

1 Experimental procedure

The samples were grown on (100)-oriented InP epi-ready substrates by a VG Semicon V80H gas source molecular beam epitaxy (GSMBE) system. The elemental gallium (Ga), In and aluminum (Al) sources were used as group III sources, and their fluxes were controlled by changing the temperatures of cells. Arsine (AsH_3) and phosphine (PH_3) cracking cells were used as group V sources, and their fluxes were controlled by adjusting the pressure. The cracking temperature was around 1000℃ measured by thermocouple. Standard beryllium (Be) and silicon (Si) effusion cells were used as p- and n-type doping sources, and the doping levels were controlled by changing the temperatures of sources. Prior to the growth, the fluxes of group III sources were calibrated by using an in situ ion gauge. The surface oxide desorption of the substrates was carried out under P_2 flux, including a slow ramp-up of the substrate temperature until the reflection high energy electron diffraction (RHEED) pattern showed an abrupt transformation to 2×4 surface reconstruction.

Two PD structures with In content of about 0.78 in the InGaAs absorption layer for the cut-off wavelength around 2.4 μm were grown. Sample (a) and (b) adopted $In_xGa_{1-x}As$ ($x=0.53$ to 0.78) and $In_xAl_{1-x}As$ ($x=0.52$ to 0.78) continuously graded buffer layers, respectively. The two epitaxy structures started from the deposition of n^+ $In_xGa_{1-x}As$ or $In_xAl_{1-x}As$ continuously graded buffer layer by controlling simultaneously the linear increase of In source temperature and decrease of Ga or Al source temperature. After that, a 2.5 μm n^- $In_yGa_{1-y}As$ absorption layer and a 0.6 μm p^+ $In_yGa_{1-y}As$ or $In_yAl_{1-y}As$ cap layer were grown. The growth rates of all layers were around 1μm/h, and the growth temperatures of the two samples measured by thermocouple were both at 530 ℃, about 30 ℃ lower than the desorption temperature of InP substrate.

The morphologies of the samples were studied using an atomic force microscope (AFM). The x-ray diffraction reciprocal space mappings (RSMs) were measured using a Philips X'pert MRD high resolution x-ray diffractometer (HRXRD) equipped with a four-crystal Ge (220) monochrometer. Cross-sectional samples were prepared for transmission electron microscopy (TEM) measurements by ion polishing and examined by a Philips CM200 FEG microscope operating at 160 kV. The PL spectra were measured using a Nicolet Megna 860 Fourier transform infrared (FTIR) spectrometer, in which liquid-nitrogen cooled InSb detector and CaF_2 beam splitter were applied. A Coherent INNOVA 305 argon-ion laser (λ = 514.5 nm) was used as an excitation source.

2 Results and discussion

The AFM images with a 40 μm × 40 μm scan area are shown in Fig. 1. A regular cross-hatch pattern was observed for these lattice-mismatched PD structures. This type of pattern could be attributed to the two types of misfit dislocations A and B oriented along the $[\bar{1}10]$

and [110] directions, corresponding to group V and III atom-based cores, respectively. Along the [$\bar{1}$10] direction, the primary ridges are in parallel, and the period of primary ridges is around 5 μm. On the ridges small periodical undulations exist and the oval-like defects pop out on the top of the ridges. The period of the small undulations is around 1 μm. The surface morphology of sample (b) appears to be more irregular than that of sample (a), which is due to the lower surface mobility of the Al atoms[6]. In spite of the difference in morphology, the root mean square (RMS) roughness values of the two samples are nearly the same with 8.2 nm and 8.7 nm for sample (a) and (b), respectively. It is inadequate to judge the qualities of the samples from morphology analysis alone. Further evaluations, such as structural and optical characterizations, are needed.

To characterize the structural properties of the samples, x-ray diffraction RSM measurements were performed for the symmetric (004) and asymmetric (224) reflections. The diffraction from the individual layers is visible, the lattice tilt (typically variable across the wafer), relaxation and composition for each individual layer can be accurately determined. The (004) and (224) RSM reflections were shown on the left side and right side of Fig. 2, respectively. The intensities are in the logarithmic scale. In all RSMs, the relatively narrow and circular peaks correspond to the InP substrate (denoted as S). In Fig. 2(a), the relatively elliptical peak corresponds to the InGaAs absorption and cap layer of sample (a) (denoted as L), with a larger diffuse scattering perpendicular to the normal line due to the existence of dislocations. In Fig. 2(b), the diffraction features from InGaAs and InAlAs individual epitaxy layers are distinguishable for the sample with InAlAs buffer. The two elliptical layer peaks correspond to the InGaAs absorption layer (denoted as L1) and InAlAs cap layer (denoted as L2) respectively. L1 and L2 were assigned by measuring the HRXRD rocking curves in the same directions before and after the etching of the InAlAs cap layer. The layer peak was shifted towards the substrate side after the etching.

On the (004) reflections, the divergencies of the centers of layer peaks and substrate peaks along the horizontal direction correspond to the macroscopic tilts of the layers to substrates. The tilt angle of InGaAs absorption layer to the substrate is −19.5° and 1.1° for sample (a) and (b), respectively. For the (224) reflections, the intensities of substrate peaks are weaker than those of layer peaks due to the thick epi-layers and the weaker diffraction intensity from asymmetric

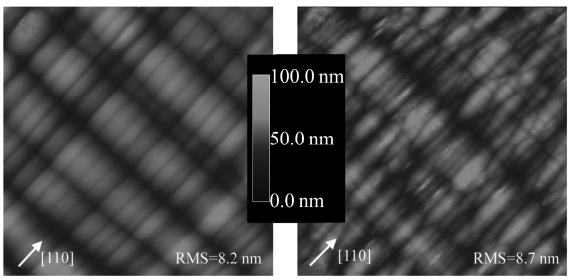

Fig. 1　AFM images of high In content InGaAs PD structures with graded (a) $In_xGa_{1-x}As$ and (b) $In_xAl_{1-x}As$ buffer layers

图 1　高 In 组分 InGaAs 探测器结构的原子力显微镜图像(40 μm×40 μm) (a) $In_xGa_{1-x}As$ 缓冲层(b) $In_xAl_{1-x}As$ 缓冲层

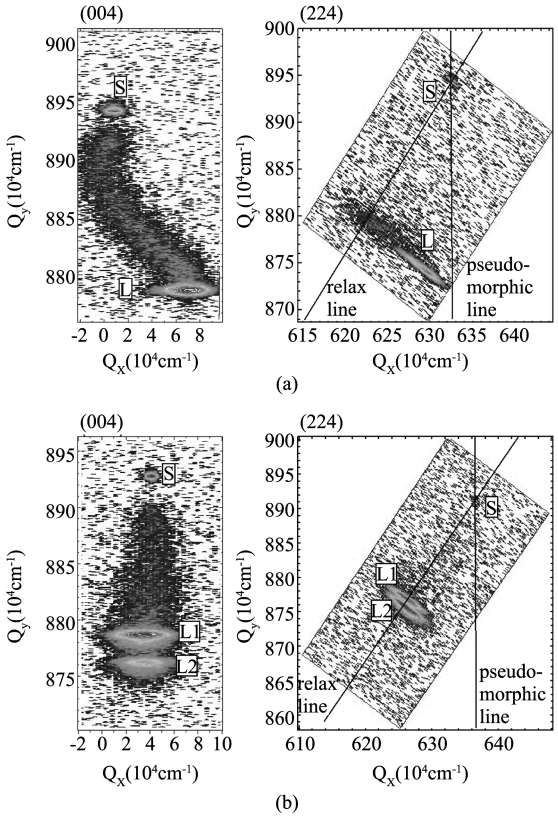

Fig. 2　RSM of high In content InGaAs PD structures with (a) $In_xGa_{1-x}As$ and (b) $In_xAl_{1-x}As$ buffer layers along (004) and (224) directions

图 2　高 In 组分 InGaAs 探测器结构的(004)和(224) 方向 RSM 图 (a) $In_xGa_{1-x}As$ 缓冲层(b) $In_xAl_{1-x}As$ 缓冲层

(224) diffraction. The parallel mismatch and perpendicular mismatch of the InGaAs absorption layer were extracted from the RSMs, and then the cubic lattice mismatch, In composition, the degrees of relaxation and residual strain of the InGaAs absorption layer have been calculated and listed in Table 1. The degrees of relaxation are both larger than 90% for sample (a) and (b). It is noted that the residual strain in sample (a) is significantly larger than the calculated value from Tersoff's model [7]. This suggests that a high tilt angle may be concurrent with a high residual strain. A possible explanation is that if the material has a significant residual strain, the lattice needs to tilt itself in order to reduce the elastic strain energy. This is consistent with the proposition of Lee et al. [8] that elastic strain can be released by lattice tilt. On the other hand, the tilt angle and residual strain of sample (b) is really slight. The real origin of the large residual strain in sample (a) is still ambiguous and needs further study.

Fig. 3 shows the dark-field TEM images of samples (a) and (b) with the (002) reflection, which is sensitive to the composition variation and dislocations. From the TEM images, we can see that the defects have been reduced significantly in InGaAs absorption layer grown on both the $In_xGa_{1-x}As$ and $In_xAl_{1-x}As$ graded buffer layers. In the graded buffer layers, most misfit dislocations are localized at the internal interfaces. Less misfit dislocations appear to propagate vertically through the structure in the $In_xAl_{1-x}As$ buffer layer than in $In_xGa_{1-x}As$ buffer layer. At the interface of $In_xGa_{1-x}As$ graded buffer and InGaAs absorption layer in sample (a), some diffraction contrast regions can be observed, which may be due to the dislocations at the interface [9]. Nevertheless, the difference of dislocation density is not so distinct in the two samples.

The optical characteristics of the samples, which are correlated to the performance of the optoelectronic device in a more straightforward way, were evaluated using PL measurements at room temperature after etching away the cap layers. As shown in Fig. 4, both of the two samples show a PL peak from InGaAs absorption layer at about 2.41 μm. Compared with sample (a), the PL intensity of sample (b) increases more than twofold at room temperature. This indicates the improved optical characteristics and less presence of non-radiation recombination centers for the PD structure with $In_xAl_{1-x}As$ graded buffer layer.

In a previous work, lower dark current and higher zero bias resistance area products R_0A have been obtained by using InAlAs heterojuction instead of InGaAs homojunction graded buffer and cap layers[10], which was attributed to the lower leakage current as a result of the wider bandgap of InAlAs. Now it is believed that the reduced residual strain and decreased non-radiation recombination centers in the PD structure with $In_xAl_{1-x}As$ graded buffer layer should be also beneficial for the improvement of device performances after the detailed characterization of material qualities.

3 Conclusion

In conclusion, GSMBE grown InP-based high In content InGaAs PD structures with In composition of about 0.78 on $In_xGa_{1-x}As$ or $In_xAl_{1-x}As$ continuously graded buffer layers have been characterized and compared. Moderate surface morphology is obtained with either $In_xGa_{1-x}As$ or $In_xAl_{1-x}As$ buffer layers, even if the PD structure with $In_xAl_{1-x}As$ buffer appears to be more irregular morphology. Nevertheless, XRD and TEM measurements show that larger residual strain is present in the PD structure with $In_xGa_{1-x}As$ buffer layer. On the other hand, only slight residual strain has

Table 1 Results from RSM measurements for InGaAs absorption layer of high In content InGaAs PD structures with continuously graded (a) $In_xGa_{1-x}As$ and (b) $In_xAl_{1-x}As$ buffer layers

表1 从采用(a)$In_xGa_{1-x}As$和(b)$In_xAl_{1-x}As$缓冲层的高In组分InGaAs探测器结构的RSM测试中提取的InGaAs吸收层参数结果

sample	parallel mismatch/%	perpendicular mismatch/%	cubic mismatch/%	In content	degree of relaxation/%	tilting angle/(°)	residual strain /(10^{-3})	
							XRD RSM	Tersoff' smodel
(a)	0.58	2.31	1.64	0.768	90.7	-19.5	-10	3.1
(b)	1.69	1.62	1.65	0.770	96.1	1.1	0.34	3.0

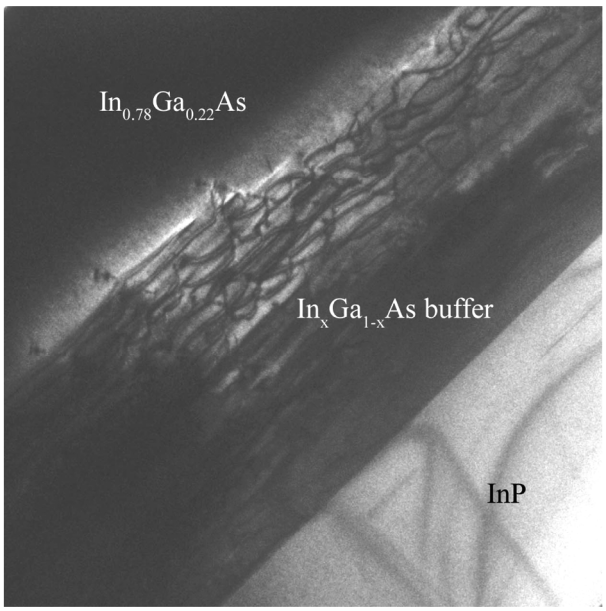

(a)

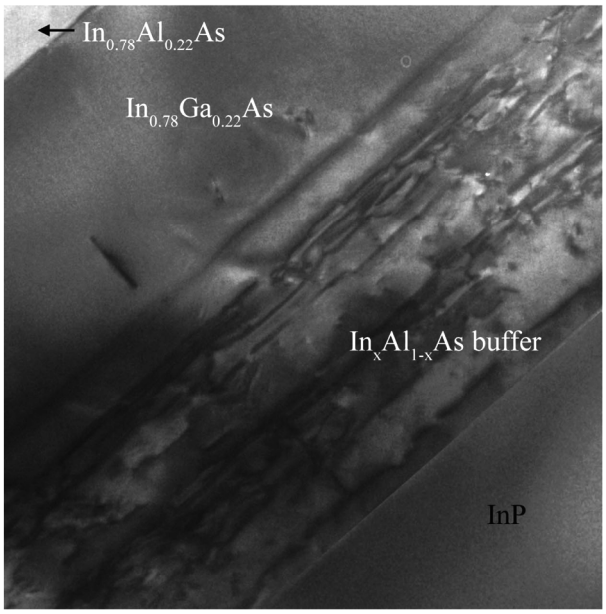

(b)

Fig. 3　Cross-sectional TEM images of high In content InGaAs PD structures with (a) $In_xGa_{1-x}As$ and (b) $In_xAl_{1-x}As$ buffer layers

图 3　高 In 组分 InGaAs 探测器结构的 TEM 截面图 (a) $In_xGa_{1-x}As$缓冲层(b) $In_xAl_{1-x}As$ 缓冲层

been observed for the PD structure with $In_xAl_{1-x}As$ buffer layer. The improved optical characteristics of the PD structure with $In_xAl_{1-x}As$ buffer layer have also been investigated. The better material quality of the PD structure with $In_xAl_{1-x}As$ graded buffer layer should be beneficial for the improvement of device performances.

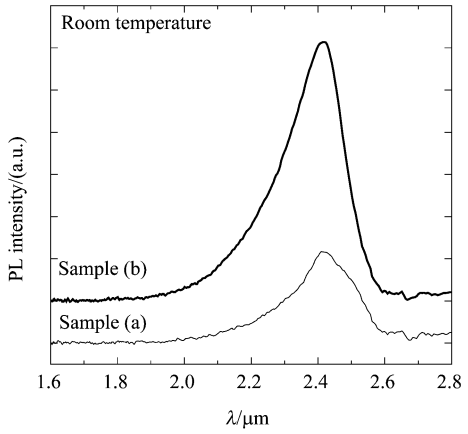

Fig. 4　PL spectra of high In content InGaAs PD structures with (a) $In_xGa_{1-x}As$ and (b) $In_xAl_{1-x}As$ buffer layers at room temperature after etching away the cap layers

图 4　高 In 组分 InGaAs 探测器在腐蚀去除帽层后的室温 PL 光谱 (a) $In_xGa_{1-x}As$ (b) $In_xAl_{1-x}As$ 缓冲层

REFERENCES

[1] Joshi A, Becker D. High-speed low-noise p-i-n InGaAs photoreceiver at 2 μm wavelength [J]. *IEEE Photonics Technol. Lett.*, 2008, **20**(8): 551 - 553.

[2] Gu Y, Li C, Wang K, *et al.* Wavelength extended InGaAs/InP photodetector structures with lattice mismatch up to 2.6% [J]. *J. Infrared Millim. Waves*, 2010, **29**(2): 81 - 86.

[3] D'Hondt M, Moerman I, Demeester P. Dark current optimization for MOVPE grown 2.5 μm wavelength InGaAs photodetectors [J]. *Electron. Lett.*, 1998, **34**(9): 910 - 912.

[4] Wada M, Hosomatsu H. Wide wavelength and low dark current lattice-mismatched InGaAs/InAsP photodiodes grown by metalorganic vapor-phase epitaxy [J]. *Appl. Phys. Lett.*, 1994, **64**(10): 1265 - 1267.

[5] Zhang Y G, Gu Y, Wang K, *et al.* Properties of gas source molecular beam epitaxy grown wavelength extended InGaAs photodectector structures on linear graded InAlAs buffer [J]. *Semicon. Sci. Technol.*, 2008, **23**(12): 125029.

[6] Chyi J I, Shieh J L, Pan J W, *et al.* Material properties of compositional graded $In_xGa_{1-x}As$ and $In_xAl_{1-x}As$ epilayers grown on GaAs substrates [J]. *J. Appl. Phys.*, 1996, **79**(11): 8367 - 8370.

[7] Tersoff J. Dislocations and strain relief in compositionally graded layers [J]. *Appl. Phys. Lett.*, 1993, **62**(7): 693 - 695.

[8] Lee D, Park M S, Tang Z, *et al.* Characterization of metamorphic $In_xAl_{1-x}As$/GaAs buffer layers using reciprocal space mapping [J]. *J. Appl. Phys.*, 2007, **101**(6): 063523.

[9] Quitoriano N J, Fitzgerald E A. Relaxed, high-quality InP on GaAs by using InGaAs and InGaP graded buffers to avoid phase separation [J]. *J. Appl. Phys.*, 2007, **102**(3): 033511.

[10] Zhang Y G, Gu Y, Tian Z B, *et al.* Performance of gas source MBE-grown wavelength-extended InGaAs photodetectors with different buffer structures [J]. *J. Cryst. Growth*, 2009, **311**(7): 1881 - 1884.